

Progress in lattice simulations for two Higgs doublet models

Guilherme Catumba,^{a,*} Atsuki Hiraguchi,^{b,g} George W.-S Hou,^c Karl Jansen,^d
Ying-Jer Kao,^{c,e} C.-J. David Lin,^{b,f} Alberto Ramos^a and Mugdha Sarkar^{b,c}

^a*Instituto de Física Corpuscular (IFIC) CSIC - Universitat de Valencia,
46071, Valencia, Spain*

^b*Institute of Physics, National Yang Ming Chiao Tung University, 1001 Ta-Hsueh Road, Hsinchu 30010,
Taiwan*

^c*Department of Physics, National Taiwan University, Taipei 10617, Taiwan*

^d*Deutsches Elektronen-Synchrotron DESY, Platanenallee 6, 15738 Zeuthen, Germany*

^e*Center for Theoretical Physics and Center for Quantum science and technology, National Taiwan
University, Taipei, 10607, Taiwan*

^f*Center for High Energy Physics, Chung-Yuan Christian University, Chung-Li 32023, Taiwan*

^g*CCSE, Japan Atomic Energy Agency, 178-4-4, Wakashiba, Kashiwa, Chiba 277-0871, Japan*

E-mail: gtelo@ific.uv.es

The custodial Two-Higgs-Doublet-Model with SU(2) gauge fields is studied on the lattice. This model has the same global symmetry structure as the Standard Model but the additional Higgs field enlarges the scalar spectrum and opens the possibility for the occurrence of spontaneous symmetry breaking of the global symmetries. Both the spectrum and the running of the gauge coupling of the custodial 2HDM are studied on a line of constant Standard Model physics with cutoff ranging from 300 to 600 GeV. The lower bounds of the realizable masses for the additional BSM scalar states are found to be well below the W boson mass. In fact, for the choice of quartic couplings in this work the estimated lower mass for one of the BSM states is found to be about $\sim 0.2m_W$ and independent of the cutoff.

*The 41st International Symposium on Lattice Field Theory,
July 28th to August 3rd, 2024,
University of Liverpool, United Kingdom*

*Speaker

1. Introduction

The standard model (SM) has been very successful in explaining experimental results. However, searches for physics beyond the SM (BSM) are important and should be pursued, with one of the key motivations being the need of a strong first-order electroweak phase transition (EWPT) in the theory of electroweak baryogenesis. It has been known that the SM does not facilitate such a phase transition at the measured Higgs boson mass, $m_h \approx 125$ GeV [1, 2].

The simplest BSM extension complying with the observations is the *two-Higgs-doublet model* (2HDM), where a second $SU(2)$ -doublet scalar field is added to the theory. This model yields an enlarged spectrum and also rich phenomenology. Dark matter candidates within the 2HDM-type, usually called *inert double models*, were proposed in [3–5]. Moreover, 2HDMs are also an important part of many supersymmetric theories such as the Minimal Supersymmetric Standard Model [6, 7].

The Lagrangian of the 2HDM considered in this work contains the kinetic terms of both scalar and gauge fields, and the most general $SU(2)$ -invariant scalar potential. Since we are interested in the lattice application, from now on we consider the case of real couplings only. This is the CP-conserving 2HDM [8, 9]. With this choice, the most general renormalizable 2HDM scalar potential has 10 real parameters, and in the usual doublet formulation reads

$$V_{2\text{HDM}} = \mu_{11}^2 \phi_1^\dagger \phi_1 + \mu_{22}^2 \phi_2^\dagger \phi_2 + \mu_{12}^2 \text{Re}(\phi_1^\dagger \phi_2) + \lambda_1 (\phi_1^\dagger \phi_1)^2 + \lambda_2 (\phi_2^\dagger \phi_2)^2 + \lambda_3 (\phi_1^\dagger \phi_1) (\phi_2^\dagger \phi_2) + \lambda_4 (\phi_1^\dagger \phi_2) (\phi_2^\dagger \phi_1) + \lambda_5 \text{Re}(\phi_1^\dagger \phi_2)^2 + \text{Re}(\phi_1^\dagger \phi_2) \left[\lambda_6 (\phi_1^\dagger \phi_1) + \lambda_7 (\phi_2^\dagger \phi_2) \right]. \quad (1)$$

The amount of literature on the 2HDM is vast and on-going (see ref. [10] and references therein). Most of the works focus on a perturbative, tree-level analysis of the theory. On the other hand, the lattice studies of the 2HDM are scarce [11, 12] and a thorough non-perturbative analysis is needed. Furthermore, recent investigations suggest that large self interacting couplings in the BSM sector may be realizable within the SM bounds [13, 14]. In fact, finite-temperature studies indicate that baryogenesis in 2HDM may benefit from large couplings [15–18], such that the electroweak phase transition is of strong first-order in this regime. Two aspects are of importance: the study of the spectrum of the theory, and the non-perturbative analysis of the finite-temperature transition, both of which have not been explored by lattice simulations, and are covered in this work.

In this work we take the \mathbb{Z}_2 -breaking terms in eq. (1) to vanish, $\mu_{12} = \lambda_6 = \lambda_7 = 0$, defining the so-called *inert models*. Moreover, by imposing the condition $\lambda_4 = \lambda_5$ we obtain the custodial limit of the 2HDM. In this case the symmetry structure is identical to the SM, with the action being invariant under global $SU(2)$ transformations where both fields transform simultaneously.

The lattice action for the custodial 2HDM used in this work can then be written as

$$S_{2\text{HDM}} = \sum_x \sum_{n=1}^2 \left\{ \sum_{\mu} -2\kappa_n \text{Tr} \left(\Phi_n^\dagger U_{\mu} \Phi_n(x + \mu) \right) + \text{Tr} \left(\Phi_n^\dagger \Phi_n \right) + \eta_n \left[\text{Tr} \left(\Phi_n^\dagger \Phi_n \right) - 1 \right]^2 \right\} + 2\mu^2 \text{Tr} \left(\Phi_1^\dagger \Phi_2 \right) + \eta_3 \text{Tr} \left(\Phi_1^\dagger \Phi_1 \right) \text{Tr} \left(\Phi_2^\dagger \Phi_2 \right) + 2\eta_4 \text{Tr} \left(\Phi_1^\dagger \Phi_2 \right)^2 + S_{\text{YM}}, \quad (2)$$

where $S_{\text{YM}} = \beta \sum_x \sum_{\mu > \nu} \left[1 - \frac{1}{2} \text{Re} \text{Tr} U_{\mu\nu}(x) \right]$ is the standard Wilson plaquette action with $U_{\mu\nu}$ being the plaquette and $\beta = 4/g^2$.

In this formulation we consider the quaternion formalism, where scalar fields in the fundamental representation of $SU(2)$ are written as a matrix, $\Phi_n(x) = \frac{1}{\sqrt{2}} \sum_{\alpha=1}^4 \theta_\alpha \varphi_n^\alpha(x)$ with φ_n^α being real components, $\alpha = 1, 2, 3, 4$, $\theta^4 = \mathbb{1}_{2 \times 2}$, and $\theta^k = i\sigma^k$ for $k = 1, 2, 3$ with σ^k being the Pauli matrices. In this representation the fields Φ_n transform under the $SU(2)$ gauge group by a left multiplication, and under the global $SU(2)$ by right multiplication, $\Phi_n \rightarrow L(x)\Phi_n R$.

2. Phase structure & spectrum

While the single Higgs doublet model, governed by three bare couplings, has a simple phase structure¹, the enlarged parameter space of the 2HDM complicates the phase structure.

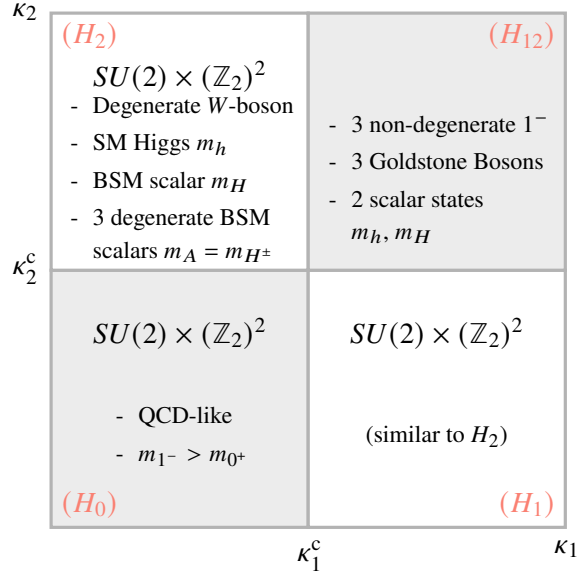


Figure 1: Summary of the cutodial 2HDM parameter space with the global symmetries and spectrum content for each of the sectors H_0, H_1, H_2, H_{12} .

In the case of the inert models, it is possible to divide the parameter space in four different regions where none, one, or both scalar fields are in the Higgs phase [10]. In the perturbative formulation, using the vacuum expectation values, v_i , for each scalar field this corresponds to: $(H_0) : v_1 = v_2 = 0$, $(H_2) : v_1 = 0, v_2 \neq 0$, $(H_1) : v_1 \neq 0, v_2 = 0$, $(H_{12}) : v_1 \neq 0, v_2 \neq 0$. These sectors divide the κ_1, κ_2 plane into four regions defined by the critical values, κ_i^c . Note, however, that not all four can be seen as separate phases since some of these transitions are crossovers for certain regimes of the couplings. The global symmetries and predicted particle content of each of the phases are summarized in fig. 1.

Sectors (H_1) , (H_2) , and (H_{12}) have the Higgs mechanism active. However, the custodial $SU(2)$ symmetry is spontaneously broken in (H_{12}) . The absence of the custodial symmetry, and the presence of massless Goldstone bosons in the spectrum exclude this phase from phenomenological considerations, since a viable 2HDM has to reproduce SM physics at low energies.

¹In fact, only a single phase exists in the Higgs-gauge interaction. The confinement and Higgs phases are analytically connected.

Sectors (H_1) and (H_2) are equivalent, and for definitiveness we will work with the latter. This is defined by $\kappa_2 > \kappa_2^c$, $\kappa_1 < \kappa_1^c$, and consequently, it is the field Φ_2 that reproduces the SM-like Higgs. At tree-level this model predicts the existence of three degenerate scalar particles, $m_A^2 = m_{H^\pm}^2 = \mu_{11}^2 + \lambda_3 v^2/2$, and two other scalar states, $m_H^2 = m_{H^\pm}^2 + \lambda_4 v^2$, and $m_h^2 = \mu_{22}^2 v^2$, the latter being identified with the SM Higgs.

On the lattice the spectrum is obtained in sector (H_2) by studying the large time behavior of two-point functions $\langle O(t)O(0) \rangle$, where O is a zero momentum composite operator with the quantum number of the particle of interest. In particular we investigate the following operators,

$$S_{ij}^a(x^4) = \sum_{\vec{x}} \text{Tr} \left[\Phi_i^\dagger(x) \Phi_j(x) \theta^\alpha \right], \quad W_{ij,\mu}^a(x^4) = \sum_{\vec{x}} \text{Tr} \left[\Phi_i^\dagger(x) U_\mu(x) \Phi_j(x + \hat{\mu}) \theta^\alpha \right]. \quad (3)$$

In sector (H_2) the assignment between the interpolators and the spectrum is: S_{22} sources the SM Higgs, and W_{22}^j the W bosons; S_{12}^4 or W_{12}^4 source the scalar state H , and S_{12}^j or W_{12}^j the scalar states A and H^\pm .

3. Standard model physics

In order to study the cutoff dependence of the enlarged spectrum of the theory we must define a line of constant physics. Since we are interested in performing a non-perturbative study of the BSM scalar states in the 2HDM, and given that only SM physics is available, we build a line of partially constant physics (LPCP). The Higgs sector of the SM has two independent dimensionless renormalized quantities that can be conveniently defined for the LPCP. Namely, the ratio of the Higgs to the W boson masses, $R \equiv \frac{m_h}{m_W}$ and the renormalized running gauge coupling $g_R^2(\mu)$. In the following, we fix the R -ratio to be close to the SM value, $R \approx 1.5$, while the renormalized gauge coupling is set to its physical value at the scale of the W boson mass, $g_R^2(\mu = m_W) \equiv 4\pi a_W \sim 0.5$.

The definition of the renormalized running gauge constant is done through the gradient flow action density [19],

$$\langle E(x, t) \rangle = -\frac{1}{4} \langle G_{\mu\nu}^a(x, t) G_{\mu\nu}^a(x, t) \rangle, \quad (4)$$

where $G_{\mu\nu}(x, t) = \partial_\mu B_\nu(x, t) - \partial_\nu B_\mu(x, t) + [B_\nu(x, t), B_\mu(x, t)]$ is the flowed gauge field strength. On the lattice we use the Clover discretization of the field strength tensor and the Wilson action for the discretized flow equation.

Using the relation between the renormalized gauge coupling at the scale $\mu = 1/\sqrt{8t}$ and the flowed action density [20], we define the gradient flow renormalized gauge coupling by

$$g_{GF}^2(\mu) \equiv \frac{128\pi^2}{9} t^2 \langle E(t) \rangle \Big|_{t=1/8\mu^2}, \quad g_{GF}^2(\mu = m_W) = 0.5, \quad (5)$$

where $\langle E(t) \rangle$ is obtained from the Euclidean spacetime average of $\langle E(x, t) \rangle$. On the lattice this condition is equivalent to $S \equiv \sqrt{8t_0} m_W = 1.0$ where the flow scale t_0/a^2 is defined by eq. (5).

4. Results

The adopted strategy to build the LPCP is to sequentially increase the bare coupling β towards the continuum while scanning the $\{\kappa_2, \eta_2\}$ -space to find parameters such that the above SM conditions are satisfied.

β	8.2	8.3	8.4	8.56	8.64
κ_2	0.13175	0.13104	0.1306	0.1301	0.129985
η_2	0.00338	0.003	0.00285	0.00275	0.002737
R	1.509(94)	1.527(80)	1.494(65)	1.504(39)	1.462(53)
S	1.0055(98)	0.9956(65)	0.994(14)	0.994(20)	0.9958(94)
am_h	0.402(28)	0.363(21)	0.305(16)	0.2192(84)	0.1863(75)
am_W	0.2666(26)	0.2377(15)	0.2041(29)	0.1458(29)	0.1275(11)
t_0/a^2	1.7781(58)	2.1934(74)	2.966(13)	5.810(45)	7.626(43)
Λ (GeV)	301.5(29)	338.2(21)	393.8(57)	551(11)	630.4(56)
$m_W L$	8.485(14)	7.639(13)	6.569(15)	4.694(18)	6.145(17)

Table 1: Bare couplings β , κ_2 , η_2 of the LPCP together with the corresponding physical conditions R , S , the SM masses am_h , am_W in lattice units, the gradient flow scale t_0/a^2 and the estimated cutoff energy Λ_c . The remaining couplings were fixed to the values: $\kappa_1 = 0.1245$; $\eta_1 = 0.003$; $\eta_3 = 0.002$; $\eta_4 = \eta_5 = 0.0001$. The simulations were performed on lattices with $L = 28, 28, 32, 32, 48$.

In this strategy the remaining degrees of freedom of the theory are kept fixed, namely the value of the BSM bare couplings ($\kappa_1, \eta_1, \eta_3, \eta_4$) are chosen such that the additional masses m_H and $m_A = m_{H^\pm}$ are larger than the SM masses but well below the lattice cutoff. Finally, the couplings η_3, η_4 were chosen to be small. In this way, the LPCP in the SM sector should be mostly insensitive to the Φ_1 scalar sector. Notice that while the initial strategy keeps the BSM bare couplings constant, later we will explore the effect of the BSM couplings.

The results for the tuning of the LPCP defined by β, κ_2, η_2 are shown in table 1. Five β values were considered, with the cutoff ranging from 300 GeV to 630 GeV. The scale setting is obtained from the physical value $m_W^{\text{phys}} = 80.377(12)$ GeV [21] with $a = \hat{m}_W/m_W^{\text{phys}}$, where \hat{m} is the mass in lattice units. Both the physical conditions R, S , and the lattice cutoff $\Lambda = 1/a$ are shown in fig. 2 as a function of am_W and β , respectively.

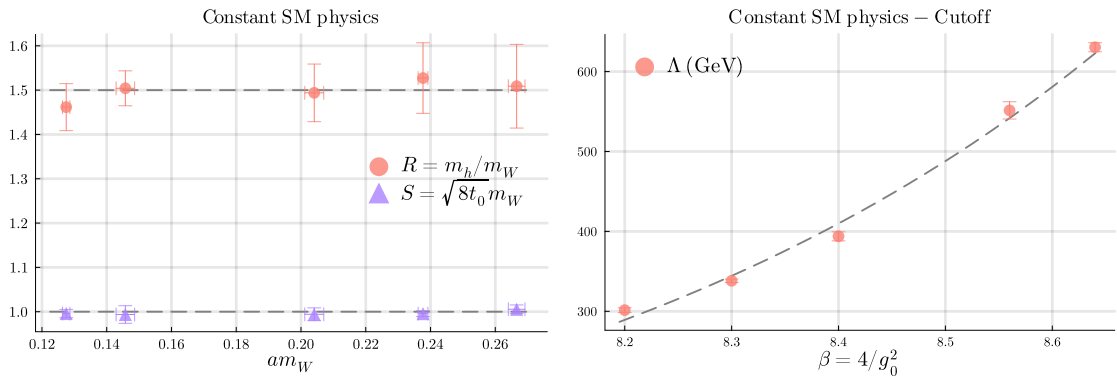


Figure 2: Data from table 1: physical conditions R and S for the selected points in the line of constant SM physics as a function of am_W (left). For decreasing am_W , each point has a corresponding increasing β value. The lattice cutoff, $\Lambda = 1/a$, estimated from $a = \hat{m}_W/m_W^{\text{phys}}$ is shown on the right as a function of β .

The gradient flow running of the gauge coupling was computed for each point in table 1. The

results for $g_{GF}^2(\mu = 1/\sqrt{8t}; \beta)$ are shown in fig. 3 as a function of the energy scale relative to m_W . All curves match for a large range, with lattice artifacts being only apparent for large values of μ .²

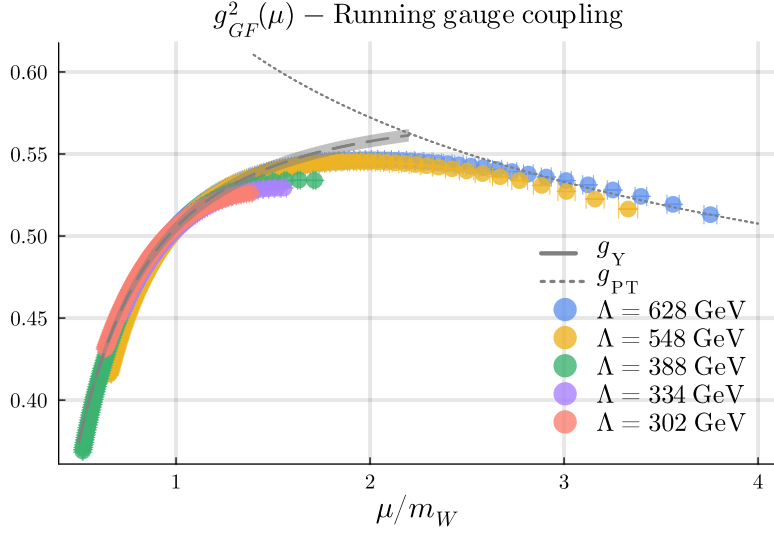


Figure 3: Running gauge coupling $g_{GF}^2(\mu)$ as a function of μ/m_W from lattice simulations along the LPCP in table 1. Only scales with $\sqrt{8t}/a > 2$ are shown. The perturbative result is matched to the curve corresponding to $\Lambda = 628$ GeV. The gauge coupling from the Yukawa potential is fitted to the infrared region, with the estimated screening mass $m_{\text{screen}} = 0.6243(28)m_W$.

In fig. 3 the perturbative result, g_{PT}^2 is also shown for large energies. This was computed from the one-loop β -function $\beta_{SU(N)+\text{Scalars}} = \mu \frac{dg}{d\mu} = -\frac{b_0 g^3}{16\pi^2} + \mathcal{O}(g^5)$, with $b_0 = \frac{11N - n_s}{3}$, and $n_s = 2$ is the number of scalar fields and $N = 2$. The matching between the massive non-perturbative and the massless perturbative schemes was done at a large enough energy scale, $\mu \approx 3.5m_W$.

From fig. 3 the structure of the running can be understood as follows: for energies $\mu \gg m_W$ the gauge boson is effectively massless, and, the gauge coupling decreases as we increase the scale, showing QCD-like asymptotic freedom. For energies $\mu \gtrsim m_W$, the mass of the W becomes relevant and the coupling stops increasing. The screening of the gauge force due to the massive W boson is clear from the difference between the perturbative and the non-perturbative result. For $\mu \ll m_W$, the gauge boson decouples and we effectively recover a scalar theory.

It is also interesting to explore the infrared structure of the running gauge coupling. For this reason, a coupling $g_Y^2(\mu = 1/r) = r^2 \frac{dV_Y}{dr}$ from a Yukawa-like potential [22, 23], $V_Y(r) \propto \frac{1}{r} e^{-mr}$ was fit to the lattice data in fig. 3. The results of the fit for the finest lattice is shown in fig. 3, with the corresponding Debye screening-mass estimated³ as $m_{\text{screen}} = 0.6243(28)m_W \approx 50$ GeV.

While the points the LPCP have the SM observables fixed to their physical values, the BSM couplings remain as free parameters. A particularly interesting objective would be to establish non-perturbative bounds on the BSM spectrum, which would require a scan over the whole parameter

²For each curve, only energies below a certain threshold are shown, corresponding to flow time radius $\sqrt{8t}/a > 2$, that correspond to $t/a^2 > 0.5$. Smaller flow times lead to large lattice artifacts.

³Since we are using a fixed form $e^{-m/\mu}$ for the Yukawa potential the arbitrariness in the definition of the renormalized running coupling, and the scale at which it is defined would lead to different screening-masses.

space. Instead, keeping the quartic couplings small, we explore the effect of changing the ‘unbroken’ hopping parameter κ_1 within the sector (H_2).

We performed simulations at different κ_1 values within sector (H_2) for each β in table 1. The SM conditions were monitored for each simulation, and the results are summarized in the left plot of fig. 4. Within the available precision the physical conditions remain roughly unchanged by the change in κ_1 .

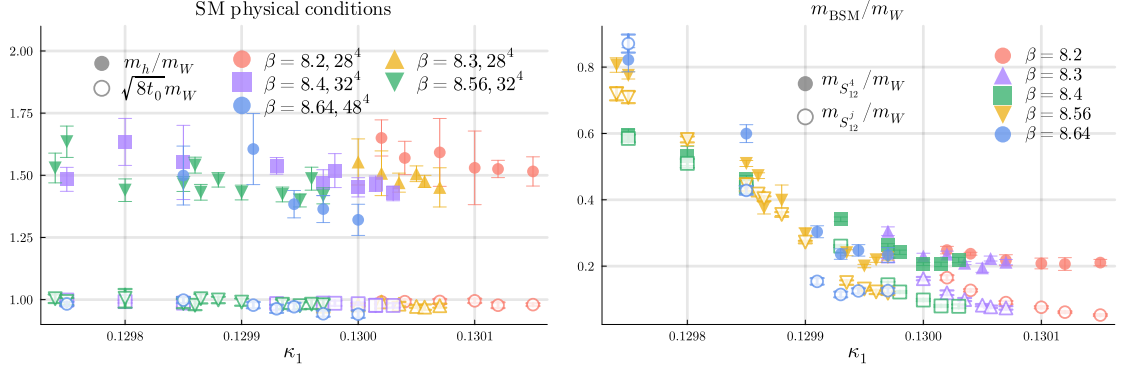


Figure 4: Left: Standard Model conditions for simulations at different κ_1 with the remaining couplings defined in table 1. Right: mass ratio between the BSM states, $m_{S_{12}^4} = m_H$, $m_{S_{12}^j} = m_A = m_{H^\pm}$, and the W boson mass, m_W , for the same points at different κ_1 below (H_{12}).

The mass ratios of the BSM states with the W boson are shown in fig. 4 for all β values in the LCPC. The improved precision allows us to observe the mass-gap between the H and the A, H^\pm states. While the mass ratio m_H/m_W develops a plateau when approaching κ_1^c from below, indicating a saturation to a finite value before the transition into (H_{12}), the ratio $m_A/m_W = m_{H^\pm}/m_W$ seems to keep decreasing with increasing κ_1 .

In the following we discuss our work on the finite temperature transitions in this model. The points of the LPCP were simulated using asymmetric lattices, with the temporal extent defining the physical temperature by $T = 1/(aL_4)$. The ‘symmetry restoration’ that deactivates the Higgs mechanism can be observed in the global observable L_{α_2}

$$L_{\alpha_2} = \frac{1}{8V} \sum_{x,\mu} \text{Tr} \left\{ \alpha_2^\dagger(x) U_\mu(x) \alpha_2(x + \hat{\mu}) \right\}, \quad (6)$$

where α_n is the ‘angular’ part of the quaternion Higgs field, $\Phi_n = \rho_n \alpha_n$, $\rho_n \in \mathbb{R}$, $\alpha_n \in SU(2)$. In the left plot of fig. 5 the renormalized ratio $L_{\alpha_2}(T, g)/L_{\alpha_2}(0, g)$ (g denotes all couplings) is shown as a function of the dimensionless ratio m_W/T with am_W taken from the zero temperature simulations. Lattice artifacts can be seen at high energies due to the use of very small temporal extents.

The departure of $L_{\alpha_2}(T)/L_{\alpha_2}(0)$ from unity at high temperatures signals the passage to the ‘symmetric’ confinement region (H_0), around $m_W/T_c \sim 0.5$, with T_c the critical temperature. In order to better resolve the transition point, and to understand the character of this phase transition we compute the susceptibility by $\chi(L) = L^4 \left(\langle L_\alpha^2 \rangle - \langle L_\alpha \rangle^2 \right)$. This is shown for L_{α_2} in the right plot of fig. 5 for the two finest lattices and different spatial volumes. The absence of volume dependence

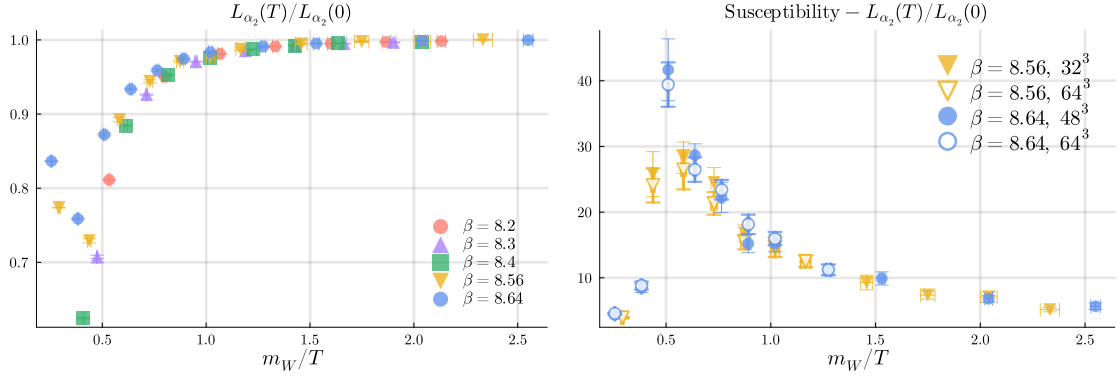


Figure 5: Finite temperature dependence of the ratio $O(T, g)/O(0, g)$ (left) and $\chi_O(T, g)/\chi_O(0, g)$ (right) for $O = L_{\alpha_2}$. The susceptibility is shown only for the two largest β values and for different spatial volumes are shown.

in the peak of the susceptibility indicates that, similarly to the single Higgs case, the electroweak transition in the weakly coupled 2HDM is a crossover.

5. Conclusion

We have studied the inert and custodial limit of the 2HDM along a line of constant SM physics defined in the Higgs sector of the theory with the unbroken $SU(2)$ custodial symmetry. Both the Higgs-to-W mass ratio, and the renormalized weak gauge coupling at the mass scale of the W boson were fixed to their physical values in order to define a LPCP.

The running of the gauge coupling, computed with the gradient flow scheme along the LPCP, defines a single curve for a large range of energies. This was compared with the one-loop massless scheme at high energies, and with a Yukawa potential at low energies.

A scan in the BSM sector was performed with constant SM physics, allowing to probe different regions of the parameter space. We have found that very light ($m_H \sim 0.2m_W$) BSM scalar states are realizable within the LPCP tuned at weak quartic couplings.

The finite temperature transition was also studied along the LPCP. The results show a transition occurring around $m_W/T_c \sim 0.5$ for the finest β values. However, only the finest two lattices allow the observation of a well defined peak in the susceptibility. The lack of volume dependence in the latter indicates a smooth crossover behavior at small quartic couplings for the electroweak phase transition, which is in agreement with most of the perturbative tree-level predictions.

The use of small BSM quartic couplings have been particularly helpful in this work. As indicated before, they make the BSM sector roughly independent of the SM physics, and prevent the need of retuning the LPCP when scanning the BSM sector. While this is an advantage from the computational perspective, there is no fundamental reason for the choice of small couplings, and a complete study is necessary in the future. In fact, $O(1)$ quartic couplings are thought to be required for a strong first-order electroweak phase transition. Tree-level results [17, 18] indicate the need of large mass splitting within the BSM scalar sector for the occurrence of a strong first-order transition. This condition directly relates to an enhanced value of the inter-flavour Higgs quartic couplings, namely η_3 .

Acknowledgements

The authors acknowledge financial support from the Generalitat Valenciana (genT program CIDEAGENT/2019/040), Ministerio de Ciencia e Innovacion (PID2020-113644GB-I00), the Academic Summit Project – NSTC 112-2639-M-002-006-ASP of Taiwan. GC, CJDL, and AR acknowledge the CSIC-NSTC exchange grant 112-2927-I-A49-508. CJDL acknowledges the financial support from NSTC project 112-2112-M-A49-021-MY3. Similarly, GWSH, CJDL and MS acknowledge the support from the NSTC project 112-2639-M-002-006-ASP.

References

- [1] H.G. Evertz, J. Jersak and K. Kanaya, *FINITE TEMPERATURE SU(2) HIGGS MODEL ON A LATTICE*, *Nucl. Phys. B* **285** (1987) 229.
- [2] M. D’Onofrio and K. Rummukainen, *Standard model cross-over on the lattice*, *Physical Review D* **93** (2016) .
- [3] E. Ma, *Verifiable radiative seesaw mechanism of neutrino mass and dark matter*, *Phys. Rev. D* **73** (2006) 077301 [[hep-ph/0601225](#)].
- [4] R. Barbieri, L.J. Hall and V.S. Rychkov, *Improved naturalness with a heavy higgs boson: An alternative road to cern lhc physics*, *Physical Review D* **74** (2006) .
- [5] L.L. Honorez, E. Nezri, J.F. Oliver and M.H.G. Tytgat, *The Inert Doublet Model: an Archetype for Dark Matter*, *J. Cosmol. Astropart. Phys.* **2007** (2007) 028.
- [6] H.E. Haber and G.L. Kane, *The Search for Supersymmetry: Probing Physics Beyond the Standard Model*, *Phys. Rept.* **117** (1985) 75.
- [7] H.E. Haber and R. Hempfling, *Renormalization-group-improved Higgs sector of the minimal supersymmetric model*, *Phys. Rev. D* **48** (1993) 4280.
- [8] H.E. Haber and D. O’Neil, *Basis-independent methods for the two-higgs-doublet model. iii. the cp-conserving limit, custodial symmetry, and the oblique parameters s , t , u* , *Physical Review D* **83** (2011) .
- [9] D. O’Neil, *Phenomenology of the Basis-Independent CP-Violating Two-Higgs Doublet Model [Dissertation]*, Ph.D. thesis, UC, Santa Cruz, Phys. Dept., 6, 2009. [0908.1363](#).
- [10] G. Branco, P. Ferreira, L. Lavoura, M. Rebelo, M. Sher and J.P. Silva, *Theory and phenomenology of two-Higgs-doublet models*, *Physics Reports* **516** (2012) 1.
- [11] R. Lewis and R.M. Woloshyn, *Spontaneous symmetry breaking in a two-doublet lattice Higgs model*, *Phys. Rev. D* **82** (2010) 034513.
- [12] A. Maas, *Observables in Higgsed Theories*, *Nucl. Part. Phys. Proc.* **273-275** (2016) 1604 [[1410.2740](#)].

- [13] W.-S. Hou, *Tree level $t \rightarrow ch^0$ or $h^0 \rightarrow tc$ decays*, *Physics Letters B* **296** (1992) 179.
- [14] W.-S. Hou and M. Kikuchi, *Approximate alignment in two-higgs-doublet model with extra yukawa couplings*, *Europhysics Letters* **123** (2018) 11001.
- [15] L. Fromme, S.J. Huber and M. Seniuch, *Baryogenesis in the two-Higgs doublet model*, *JHEP* **11** (2006) 038 [[hep-ph/0605242](#)].
- [16] G.C. Dorsch, S.J. Huber and J.M. No, *A strong electroweak phase transition in the 2HDM after LHC8*, *J. High Energ. Phys.* **2013** (2013) 29.
- [17] P. Basler, M. Krause, M. Muhlleitner, J. Wittbrodt and A. Wlotzka, *Strong First Order Electroweak Phase Transition in the CP-Conserving 2HDM Revisited*, *J. High Energ. Phys.* **2017** (2017) 121.
- [18] J. Bernon, L. Bian and Y. Jiang, *A new insight into the phase transition in the early Universe with two Higgs doublets*, *J. High Energ. Phys.* **2018** (2018) 151.
- [19] M. Lüscher, *Properties and uses of the wilson flow in lattice qcd*, *Journal of High Energy Physics* **2010** (2010) .
- [20] M. Lüscher and P. Weisz, *Perturbative analysis of the gradient flow in non-abelian gauge theories*, *J. High Energ. Phys.* **2011** (2011) 51.
- [21] PARTICLE DATA GROUP collaboration, *Review of Particle Physics*, *PTEP* **2022** (2022) 083C01.
- [22] W. Langguth, I. Montvay and P. Weisz, *Monte Carlo study of the standard SU(2) Higgs model*, *Nuclear Physics B* **277** (1986) 11.
- [23] Z. Fodor, J. Hein, K. Jansen, A. Jaster and I. Montvay, *Simulating the Electroweak Phase Transition in the SU(2) Higgs Model*, Sept., 1994. [10.1016/0550-3213\(95\)00038-T](#).